Human Reproduction, Vol.34, No.4 pp. 758–769, 2019
Advanced Access publication on March 6, 2019 doi:10.1093/humrep/dez012

human reproduction

ORIGINAL ARTICLE ***Reproductive genetics***

Extended *in vitro* culture of human embryos demonstrates the complex nature of diagnosing chromosomal mosaicism from a single trophectoderm biopsy

M. Popovic[1,*], L. Dhaenens[1], J. Taelman[1], A. Dheedene[2], M. Bialecka[3], P. De Sutter[1], S.M. Chuva de Sousa Lopes[1,3], B. Menten[2,†], and B. Heindryckx[1,†]

[1]Ghent-Fertility And Stem cell Team (G-FAST), Department for Reproductive Medicine, Ghent University Hospital, Corneel Heymanslaan 10, Ghent 9000, Belgium [2]Center for Medical Genetics, Ghent University Hospital, Corneel Heymanslaan 10, Ghent 9000, Belgium [3]Department of Anatomy and Embryology, Leiden University Medical Centre, Albinusdreef 2, 2333 ZA Leiden, Netherlands

*Correspondence address. Ghent-Fertility And Stem cell Team (G-FAST), Department for Reproductive Medicine, Ghent University Hospital, Corneel Heymanslaan 10, Ghent 9000, Belgium; E-mail: mina.popovic@ugent.be

Submitted on October 4, 2018; resubmitted on January 9, 2019; accepted on January 31, 2019

STUDY QUESTION: What is the accuracy of preimplantation genetic testing for aneuploidies (PGT-A) when considering human peri-implantation outcomes *in vitro*?

STUDY ANSWER: The probability of accurately diagnosing an embryo as abnormal was 100%, while the proportion of euploid embryos classified as clinically suitable was 61.9%, yet if structural and mosaic abnormalities were not considered accuracy increased to 100%, with a 0% false positive and false negative rate.

WHAT IS ALREADY KNOWN: Embryo aneuploidy is associated with implantation failure and early pregnancy loss. However, a proportion of blastocysts are mosaic, containing chromosomally distinct cell populations. Diagnosing chromosomal mosaicism remains a significant challenge for PGT-A. Although mosaic embryos may lead to healthy live births, they are also associated with poorer clinical outcomes. Moreover, the direct effects of mosaicism on early pregnancy remain unknown. Recently, developed *in vitro* systems allow extended embryo culture for up to 14 days providing a unique opportunity for modelling chromosomal instability during human peri-implantation development.

STUDY DESIGN, SIZE, DURATION: A total of 80 embryos were cultured to either 8 ($n = 7$) or 12 days post-fertilisation (dpf; $n = 73$). Of these, 54 were PGT-A blastocysts, donated to research following an abnormal ($n = 37$) or mosaic ($n = 17$) diagnosis. The remaining 26 were supernumerary blastocysts, obtained from standard assisted reproductive technology (ART) cycles. These embryos underwent trophectoderm (TE) biopsy prior to extended culture.

PARTICIPANTS/MATERIALS, SETTING, METHODS: We applied established culture protocols to generate embryo outgrowths. Outgrowth viability was assessed based on careful morphological evaluation. Nine outgrowths were further separated into two or more portions corresponding to inner cell mass (ICM) and TE-derived lineages. A total of 45 embryos were selected for next generation sequencing (NGS) at 8 or 12 dpf. We correlated TE biopsy profiles to both culture outcomes and the chromosomal status of the embryos during later development.

MAIN RESULTS AND THE ROLE OF CHANCE: Of the 73 embryos cultured to 12 dpf, 51% remained viable, while 49% detached between 8 and 12 dpf. Viable, Day 12 outgrowths were predominately generated from euploid blastocysts and those diagnosed with trisomies, duplications or mosaic aberrations. Conversely, monosomies, deletions and more complex chromosomal constitutions significantly

†These authors contributed equally to the study.

impaired *in vitro* development to 12 dpf (10% vs. 77%, $P < 0.0001$). When compared to the original biopsy, we determined 100% concordance for uniform numerical aneuploidies, both in whole outgrowths and in the ICM and TE-derived outgrowth portions. However, uniform structural variants were not always confirmed later in development. Moreover, a high proportion of embryos originally diagnosed as mosaic remained viable at 12 dpf (58%). Of these, 71% were euploid, with normal profiles observed in both ICM and TE-derived lineages. Based on our validation data, we determine a 0% false negative and 18.5% false positive error rate when diagnosing mosaicism. Overall, our findings demonstrate a diagnostic accuracy of 80% in the context of PGT-A. Nevertheless, if structural and mosaic abnormalities are not considered, accuracy increases to 100%, with a 0% false positive and false negative rate.

LIMITATIONS REASONS FOR CAUTION: The inherent limitations of extended *in vitro* culture, particularly when modelling critical developmental milestones, warrant careful interpretation.

WIDER IMPLICATIONS OF THE FINDINGS: Our findings echo current prenatal testing data and support the high clinical predictive value of PGT-A for diagnosing uniform numerical aneuploidies, as well as euploid chromosomal constitutions. However, distinguishing technical bias from biological variability will remain a challenge, inherently limiting the accuracy of a single TE biopsy for diagnosing mosaicism.

STUDY FUNDING, COMPETING INTEREST(S): This research is funded by the Ghent University Special Research Fund (BOF01D08114) awarded to M.P., the Research Foundation—Flanders (FWO.KAN.0005.01) research grant awarded to B.H. and De Snoo-van't Hoogerhuijs Stichting awarded to S.M.C.d.S.L. We thank Ferring Pharmaceuticals (Aalst, Belgium) for their unrestricted educational grant. The authors declare no competing interests.

TRIAL REGISTRATION NUMBER: N/A.

Key words: chromosomal mosaicism / preimplantation genetic testing / aneuploidy / PGT-A / PGS / post-implantation development / next generation sequencing / blastocyst outgrowth / inner cell mass / trophectoderm

Introduction

Human preimplantation development is remarkably vulnerable to error, leading to the high frequency of chromosomal abnormalities observed in human embryos. Insight into this vulnerability has been obtained following the implementation of preimplantation genetic testing for aneuploidies (PGT-A) in conjunction with ART. Aberrant chromosomal constitutions have been reported in up to 75% of Day 3 embryos (Mertzanidou *et al.*, 2013) and are as high as 50% in blastocysts (Harper *et al.*, 2012). The vast majority of these abnormalities end in implantation failure or early pregnancy loss, as observed in up to 50% of all first trimester miscarriages (van den Berg *et al.*, 2012). However, the application of next generation sequencing (NGS) for PGT-A has led to an increase in reports of chromosomal mosaicism in trophectoderm (TE) biopsies (Sachdev *et al.*, 2016; Vera-Rodriguez and Rubio, 2017). Although mosaic embryos may lead to healthy live births (Greco *et al.*, 2015; Spinella *et al.*, 2018), they have also been linked to poorer clinical outcomes compared to euploid blastocysts (Maxwell *et al.*, 2016; Munné *et al.*, 2017). However, the developmental capacity of mosaic blastocysts has thus far only been evaluated based on clinical outcome data (Greco *et al.*, 2015; Munné *et al.*, 2017; Spinella *et al.*, 2018) and no blinded, non-selection studies have been performed to assess the true predictive value of reporting mosaicism in regards to IVF outcomes. Balancing the unknown risks of transferring mosaic blastocysts with the possibility of discarding viable embryos continues to raise uncomfortable uncertainty. Nevertheless, chromosomal mosaicism is currently routinely diagnosed in many PGT-A centres worldwide. Moreover, mosaic embryos are prioritised for transfer with respect to abnormality involved, as well as the degree of mosaicism reported.

Current clinical data point to the findings of Bolton *et al.*, 2016 based on a mouse model of chromosomal mosaicism. Here, mosaic mouse blastocysts demonstrated normal developmental potential if they contained a sufficient number of euploid cells, resulting in viable, normal pups and never mosaic mice (Bolton *et al.*, 2016). However, the timing of developmental events and regulation of the cell cycle differ in mouse and human (Rossant and Tam, 2017). Additionally, the mouse model relied on artificially induced chaotic abnormalities, which are incompatible with life. It thus remains unclear whether a mosaic, single chromosome aberration, as seen in human, would lead to similar outcomes. Moreover, outcomes of mosaic trisomies leading to live birth even when present in all cells of the embryo, remain to be investigated (Munné and Wells, 2017).

Newly established embryo culture systems allow blastocyst attachment, outgrowth formation and extended culture for up to 14 days *in vitro* (Deglincerti *et al.*, 2016; Shahbazi *et al.*, 2016), providing a unique opportunity for investigating chromosomal instability during early human post-implantation development. Here, we use an extended *in vitro* embryo culture protocol to investigate the effects of chromosomal aberrations and blastocyst mosaicism on the early peri-implantation, up to 12 days post-fertilisation (dpf). While a consensus regarding the clinical management of embryo mosaicism remains difficult to attain, examining the potential implications of specific mosaic aberrations may enhance diagnosis. Moreover, evaluating chromosomal instability during these, so far, hidden stages of embryogenesis may provide valuable insights into the predictive value of reporting mosaicism in clinical practice, ultimately enhancing the embryo selection process and improving clinical outcomes.

Materials and Methods

Ethical permission

This study was approved by the Ghent University Institutional Review Board (EC2017/584) and the Belgian Federal Commission for medical and

scientific research on embryos *in vitro* (ADV_075_UZGent). All embryos used for this research were donated with patients' written informed consent, following cryopreservation.

Embryo source

Our study included blastocysts donated following PGT-A, as well as standard IVF/ICSI cycles. A total of 80 embryos from 51 patients were included in the analysis. Maternal age ranged from 23 to 42 years (with a mean of 32.84 years). PGT-A was performed within the Department for Reproductive Medicine in collaboration with the Center for Medical Genetics, Ghent University Hospital.

Blastocyst warming and biopsy

Blastocysts vitrified on Day 5 or Day 6 of development were warmed using the Vitrification Thaw kit (Irvine Scientific, Netherlands), as previously described (Van Landuyt *et al.*, 2011). Embryos were cultured in Cook Blastocyst Medium (COOK, Ireland) in 25µL drops under mineral oil (Irvine Scientific, Netherlands) at 37°C, 6% CO_2 and 5% O_2 (balance N_2). Blastocysts obtained from standard ART cycles underwent laser-assisted biopsy, as per Deleye *et al.* (2015b), prior to plating. Biopsy procedures were performed on an Olympus IX73 microscope, fitted with a LYKOS laser (Hamilton Thorne, MA, USA). To assist TE herniation, the zona pellucida was breached using a series of laser pulses, following embryo warming. Biopsied samples were processed for whole genome amplification (WGA) and subsequent NGS, as described below.

Blastocyst grading

Blastocyst quality was evaluated prior to plating using the Gardner and Schoolcraft grading criteria (Gardner and Schoolcraft, 1999).

Extended embryo culture and sample processing

All blastocysts were plated at 6 dpf. When required, embryos were briefly exposed to pre-warmed Acidic Tyrode's Solution (Sigma-Aldrich, Belgium) for removal of the zona pellucida. After washing, individual blastocysts were plated, per well, in an eight-well IbiTreat µ-plate (Ibidi, GmbH). Embryos were cultured using an *in vitro* extended culture protocol, based on previously described methods (Deglincerti *et al.*, 2016; Shahbazi *et al.*, 2016). However, all cultures were performed in hypoxic conditions (5%). Additionally, the medium was supplemented with 100 ng/mL of Activin A for the entire duration of the extended culture (6 to 12 dpf).

Of the 80 embryos plated, 54 were PGT-A blastocysts, donated to research following an abnormal ($n = 37$) or mosaic ($n = 17$) diagnosis, while the remaining 26 were supernumerary blastocysts, obtained from standard ART cycles (Fig. 1). Outgrowth viability was carefully assessed based on morphological analysis. Nine outgrowths were further separated into two or more portions, corresponding to inner cell mass (ICM) and one or more TE-derived samples. A stem cell cutting tool (Vitrolife, Sweden) was used to perform the microdissection. Both entire outgrowths and embryo portions were used for further chromosomal testing.

Next generation sequencing and analysis

We have previously shown that our NGS platform can be efficiently applied for the detection of both numerical, as well as structural chromosomal aberrations in human embryos, at a resolution of ~4.5 Mb (Deleye *et al.*, 2015a, 2015b). Moreover, we have validated our sequencing platform for the detection of mosaicism present in as low as 3 out of 10 cells, at a resolution >10 Mb (Popovic *et al.*, 2018). As such, WGA and NGS was performed as previously described (Deleye *et al.*, 2015b; Popovic *et al.*, 2018).

Per sample, our platform generated an average of ~5.5 million uniquely mapped DNA sequence reads. We have previously demonstrated that this number of reads is more than sufficient for the accurate detection of aberrations for PGT-A (Deleye *et al.*, 2015b). Our data analysis was performed using the QDNAseq algorithm, as previously described (Scheinin *et al.*, 2014). This algorithm divides the genome into fixed-sized non-overlapping windows and counts the number of sequence reads that map within each window. These counts are used to calculate a ratio to perform a median centralisation and a simultaneous two-dimensional LOESS correction for sequence mappability and GC content. Finally, these ratios are $\log_2$ transformed, ultimately resulting in the $\log_2$ relative copy numbers values (log2(CN)) used in the manuscript. The QDNAseq algorithm improves on previous methods by creating a 'blacklist' of problematic genome regions based on the ENCODE Project Consortium, particularly regions with known repeat elements, such as satellites, centromeric and telomeric repeats (Scheinin *et al.*, 2014). The QDNAseq algorithm is incorporated into the Vivar software, which we apply for further analysis (Sante *et al.*, 2014). All sequencing results were analysed in 500 kb windows, previously determined to give the best trade-off between sensitivity and specificity (Deleye *et al.*, 2015b). Analysis was restricted to aberrations >10 Mb in size and performed based on thresholds established from our NGS validation data (Popovic *et al.*, 2018). Analysis of chromosomal profiles of the outgrowths and embryo portions was performed blindly with respect to the original TE biopsy.

Immunohistochemistry

Prior to commencing the study, several viable embryos were fixed at 12 dpf with 4% paraformaldehyde for 20 min at room temperature. Embryo outgrowths were permeabilised with 0.2% Triton X-100 (Sigma-Aldrich, the Netherlands) and blocked in 10% foetal calf serum (Thermo Fisher Scientific, the Netherlands) and 1% bovine serum albumin (Sigma-Aldrich, the Netherlands). Primary antibodies used were mouse anti-POU5F1 (sc-5279, Santa Cruz, 1:250) and rabbit anti-GATA6 (sc-9055, Santa Cruz, 1:250), while secondary antibodies included Alexa Flour 555 donkey anti-rabbit (A-31572, Thermo Fisher Scientific, 1:500) and Alexa Fluor 488 donkey anti-mouse (A-21202, Thermo Fisher Scientific, 1:500). Outgrowths were counterstained with 1 µg/ml 4′,6-diamidino-2-phenylindole (DAPI, Vector Laboratories).

Embryo Imaging

Brightfield images of blastocysts and embryo outgrowths were taken on an Olympus IX73 inverted microscope (Olympus, Belgium). Fluorescence images were obtained on a Leica TCS SP8 inverted confocal microscope (Leica, Germany), equipped with a white light laser and LAS X software. Z-stack images were acquired with 2µm spacing, at Airy 1-unit pinhole, at 12 bits in 1024 × 1024 pixels and at 200 Hz laser frequency. Z-stack images were processed using Fiji (version 2.0.0-rc43/1.5k) (Schindelin *et al.*, 2012).

Statistical analysis

Fisher's Exact test (two-sided) was used for evaluating the association of blastocyst quality, as well as blastocyst chromosomal profiles and culture outcomes. Both R (v3.5.0) (R Foundation for Statistical Computing, Vienna, Austria) and GraphPad Prism (v6.01) (GraphPad Software, San Diego, CA, USA), were used for evaluating statistical significance. All *P*-values < 0.05 were considered significant.

Results

Extended embryo culture: modelling human peri-implantation *in vitro*

A total of 80, good-quality blastocysts (≥ 5BB) were plated and cultured until 8 or 12 dpf (Fig. 1, Table I). Embryos were maintained in hypoxic conditions during the entire culture period, representative of the maternal environment during peri-implantation. It has been well-established that low oxygen concentrations improve ART outcomes (Bontekoe *et al.*, 2012). Furthermore, we supplemented cultures with Activin A. Activins have been shown to be important regulators of implantation, embryogenesis and embryo viability *in vivo* (Refaat and Ledger, 2011). We validated our extended *in vitro* culture protocol prior to commencing the study, confirming phenotypes associated with early post-implantation development, including the formation of epiblast and hypoblast-like structures (Supplementary Figure S1A).

All plated blastocysts formed outgrowths by 8 dpf. Viable embryos remained attached during the *in vitro* culture and displayed morphologies comparable to early stages of cavitation, as previously described (Shahbazi *et al.*, 2016). Based on morphological analysis, we were able to confidently distinguish ICM and TE-derived phenotypes in nine embryos (Supplementary Figure S1B). Of the total embryos cultured until 12 dpf, 51% (37 out of 73) remained attached. These embryos showed good developmental progression and were viable at 12 dpf. The remaining embryos (49%) displayed considerable signs of cell death and degeneration and detached between 8 and 12 dpf (Supplementary Figure S1C). We observed no significant difference in regard to ICM nor TE quality and culture outcomes ($P = 0.6418$ and $P = 0.6378$, respectively).

Blastocysts presenting with euploid profiles, chromosomal gains and mosaicism were more likely to remain viable at 12 dpf

Of the total embryos plated from both blastocyst groups, 73 were cultured to 12 dpf (Fig. 1, Table I). Of these, 36 originally presented with either one ($n = 24$) or multiple aberrations ($n = 12$), while 18 were reported as mosaic. The latter were diagnosed with either one ($n = 10$) or multiple ($n = 2$) mosaic abnormalities, or both uniform (complete) and mosaic aberrations ($n = 6$). Additionally, 19 previously untested blastocysts were determined to be euploid (Table I).

We further correlated 12 dpf outgrowth viability to the chromosomal status of the plated blastocysts (Table I, Fig. 2). Viable 12 dpf outgrowths were predominantly generated from euploid blastocysts, as well as those diagnosed with trisomies, duplications or mosaic aberrations (34 out of 44 attached, 77%). Conversely, monosomies, deletions and chromosomal constitutions consisting of multiple aberrations, significantly impaired *in vitro* embryo development to 12 dpf (3 out of 29 attached, 10%; $P < 0.0001$) (Fig. 2).

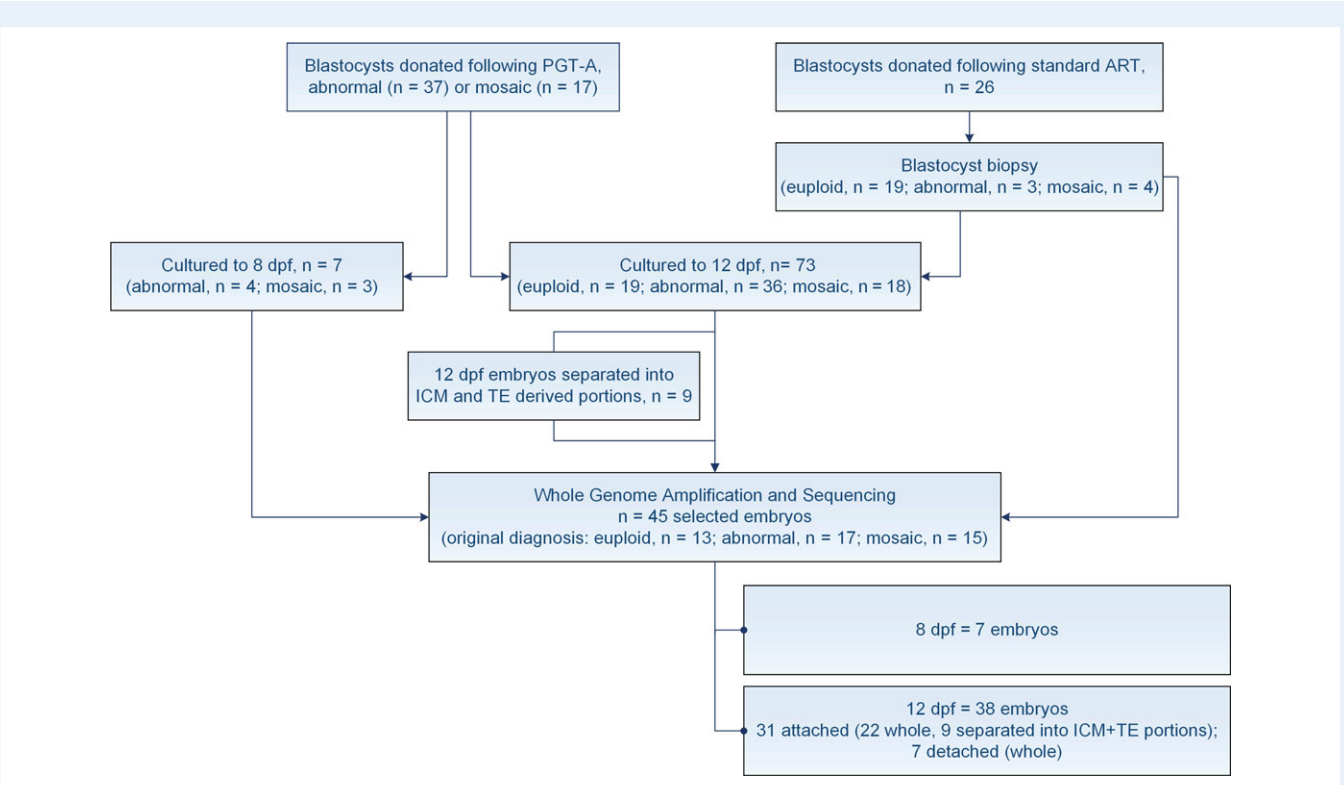

Figure 1 Study design. A total of 80 embryos were cultured for either 8 or 12 days post-fertilisation (dpf). Of these, 54 blastocysts underwent preimplantation genetic testing for aneuploidy (PGT-A) and were donated to research following an abnormal or mosaic diagnosis, while 26 were supernumerary blastocysts, obtained from standard ART cycles. The latter underwent blastocyst biopsy prior to extended culture. Nine outgrowths were further separated into inner cell mass (ICM) and trophectoderm (TE)-derived portions. A total of 45 embryos were selected for next generation sequencing (NGS) at 8 or 12 dpf.

Table I Overview of chromosomal profiles and culture outcomes for all blastocysts used in the study.

Blastocyst number	Blastocyst grade	Blastocyst profile	Outgrowth profile	Culture outcome, 12 dpf
E1	5AA	Euploid	Euploid	Attached
E2	5AA	Euploid	Euploid	Attached
E3	5AA	Euploid		Attached
E4	5BB	Euploid		Attached
E5	6AA	Euploid	Euploid	Attached
E6	6AA	Euploid	Euploid	Attached
E7	6BA	Euploid		Detached
E8	6BA	Euploid	ICM + TE derived: Euploid	Attached
E9	5AA	Euploid		Detached
E10	5BB	Euploid	Euploid	Attached
E11	5BA	Euploid	Euploid	Attached
E12	6AA	Euploid	Euploid	Attached
E13	5AB	Euploid		Detached
E14	5AA	Euploid	Euploid	Attached
E15	5BA	Euploid	Euploid	Attached
E16	5AA	Euploid	Euploid	Attached
E17	5AA	Euploid	Euploid	Attached
E18	5BB	Euploid		Attached
E19	5BB	Euploid	Euploid	Attached
PGT1	5AB	Trisomy 16	ICM + TE derived: Trisomy 16	Attached
PGT2	6AB	Trisomy 22		Attached
PGT3	5BB	Trisomy 22		Attached
PGT4	6BA	Trisomy 21	Trisomy 21	Attached
PGT5	6AA	Trisomy 22	ICM + TE derived: Trisomy	Attached
PGT6	6AB	Trisomy 19		Detached
PGT7	5AA	Trisomy 16	ICM + TE derived: Trisomy 16	Attached
PGT8	5AA	Trisomy 22	Trisomy 22	Attached
PGT9	6AA	Trisomy 22		Attached
PGT10	5BA	11q dup (17.5 Mb)	11q dup (17.5 Mb)	Attached
E20	5BA	3p dup (27.0 Mb)	Euploid	Attached
PGT11	6BB	7q dup (68.5 Mb)		Detached
PGT12	6AB	1q dup (102.0 Mb)	ICM + TE derived: Euploid	Attached
PGT13	5BA	2q del (mosaic) (72.5 Mb)	ICM + TE derived: Euploid	Attached
PGT14	5AB	3p del (mosaic) (80.5 Mb)	Euploid	Attached
PGT15	6AA	2p del (mosaic) (35.0 Mb)	Euploid	Attached
PGT16	5AA	Monosomy 14 (mosaic)		Detached
E21	5AB	Trisomy 3 (mosaic)	ICM + TE derived: Trisomy 3	Attached
E22	5AB	7q del (mosaic) (18.0 Mb)		Detached
PGT17	5BB	Monosomy 18 (mosaic)		Detached
E23	5BA	Trisomy 4 (mosaic)	Monosomy 4 (mosaic)	Attached
PGT18	5BB	Monosomy 7 (mosaic)	Monosomy 7	Detached
PGT19	6AA	Trisomy 5 (mosaic)	ICM + TE derived: Euploid	Attached
PGT20	6BB	Trisomy 11 (mosaic), 9q dup (mosaic) (69.5 Mb)	Euploid	Attached
PGT21	5AA	Trisomy 20 (mosaic), Monosomy 14 (mosaic)		Detached
PGT22*	6BB	Trisomy 1 (mosaic), Trisomy 16 (mosaic)	Euploid	
E24	6BA	Monosomy 2, Monosomy 1 (mosaic)		Detached

Continued

Table I *Continued*

Blastocyst number	Blastocyst grade	Blastocyst profile	Outgrowth profile	Culture outcome, 12 dpf
PGT23	5AB	Trisomy 11, Monosomy 3 (mosaic)	Trisomy 11	Detached
PGT24	5BA	Monosomy 21, 7q del (mosaic) (65.5 Mb)		Detached
PGT25	5AB	Monosomy 16, Trisomy 15 (mosaic)	Monosomy 16	Detached
PGT26	5AA	Monosomy 22, Trisomy 5 (mosaic)	Monosomy 22	Attached
PGT27	5BB	Trisomy 21, Trisomy 22, 5p dup (mosaic) (141.0 Mb), 5q del (mosaic) (39.0 Mb)	ICM + TE derived: Trisomy 21, 22	Attached
PGT28*	5AB	1p dup (118.5 Mb), 6q dup (mosaic) (55.5 Mb)	1p dup (118.5 Mb)	
PGT29*	6AA	11q dup (79.0 Mb), 11p del (mosaic) (47.5 Mb)	Euploid	
PGT30	5BA	Monosomy 14		Detached
PGT31	5AA	Monosomy 8		Detached
PGT32	5AA	Monosomy 2		Detached
PGT33	5BB	Monosomy 10		Detached
PGT34	5BA	Monosomy 14		Detached
E25	5BA	Monosomy 16	Monosomy 16	Attached
PGT35*	5AA	Monosomy 13	Monosomy 13	
PGT36	5BB	Monosomy 4	Monosomy 4	Detached
PGT37	6AA	Monosomy 22		Detached
PGT38	5BB	Monosomy 9		Detached
PGT39	6AA	Monosomy 16		Detached
PGT40	5BA	10q del (22.0 Mb)	10q del (22.0 Mb)	Detached
PGT41*	5AB	1p del (118.0 Mb)	1p del (118.0 Mb)	
PGT42	5BA	Trisomy 15, Trisomy 21	Trisomy 15, Trisomy 21	Detached
PGT43	5BB	Trisomy 5, Trisomy 15	Trisomy 5, Trisomy 15	Detached
PGT44	6AB	Chaotic profile		Detached
E26	6AA	Chaotic profile		Detached
PGT45	5BA	Trisomy 13, Monosomy 21, 16p del (20.5 Mb)		Detached
PGT46	5AA	2q dup (54.0 Mb), 3p del (72.0 Mb)		Detached
PGT47	6AA	1q del (36.0 Mb), 20p dup (28.0 Mb)		Detached
PGT48	5AA	1q del (36.0 Mb), 20p dup (28.0 Mb)		Detached
PGT49	5BB	Trisomy 16, 2p del (187.5 Mb), 3p dup (125.5 Mb)		Detached
PGT50	5BB	Monosomy 5, Monosomy 22		Detached
PGT51	5BA	Monosomy 18, Monosomy 22		Detached
PGT52	5AB	Monosomy 7, Trisomy 15		Detached
PGT53*	5BB	Monosomy 4, Trisomy 19	Monosomy 4, Trisomy 19	
PGT54*	6AA	3q del (74.5 Mb), 10q dup (30.5 Mb)	3q del (74.5 Mb), 10q dup (30.5 Mb)	

Embryo numbers starting with 'E' denote blastocysts donated following standard ART cycles. Embryo numbers starting with 'PGT' denote blastocysts donated following PGT-A. Embryos cultured until 8 days post-fertilisation are indicated with (*). dup = duplication, del = deletion, Mb = megabase.

Sensitivity and specificity of NGS for detecting chromosomal mosaicism

We have previously demonstrated that SurePlex amplified samples show a high overall accuracy for calling copy number variations (CNVs; Deleye *et al.*, 2015a). Nevertheless, representation bias, particularly of GC-content rich genomic regions is known to hinder NGS analysis (Capalbo *et al.*, 2017). In addition, we have shown that the size of the aberration has a major impact on the likelihood that its $\log_2$ relative copy number value will lie outside the determined thresholds for calling CNVs (Deleye *et al.*, 2015a; Popovic *et al.*, 2018). We previously validated our sequencing platform for the detection of mosaicism present in as low as 3 out of 10 cells, at a resolution >10 Mb (Popovic *et al.*, 2018). We further used this data to examine the sensitivity and specificity of detecting mosaicism with our approach (Goodrich *et al.*,

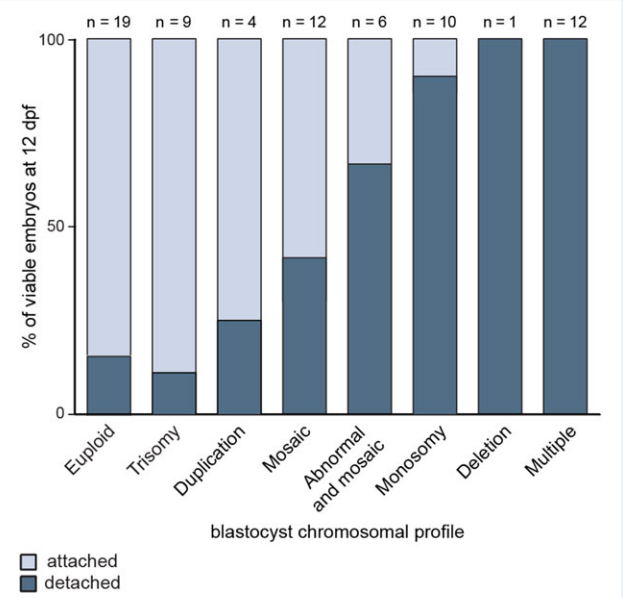

Figure 2 Blastocyst chromosomal profiles related to culture outcomes. Euploid blastocysts and those presenting with chromosomal gains and mosaicism were significantly more likely to remain viable 12 days post-fertilisation (dpf), compared to blastocysts with chromosomal losses or multiple aberrations.

2017). Samples were blinded and reassessed. Results were then evaluated for consistency with the expected chromosomal constitutions, taking into account pre-determined thresholds for calling mosaicism. Sensitivity, the ratio of samples determined to be abnormal for the correct chromosome was 100% (21 out of 21), with a 0% false negative error rate. Furthermore, specificity, the proportion of samples accurately diagnosed as euploid for all chromosomes expected to be normal, was determined to be 81.5% (22 out of 27), with a 18.5% false positive error rate.

Uniform numerical aneuploidies and euploid profiles were always verified later in development, but structural variants were not always concordant

We determined 100% concordance between uniform numerical aneuploidies diagnosed at the blastocyst stage and at both 8 and 12 dpf (Table I). This applied to whole outgrowths and those for which lineage-specific profiles were obtained (Table I, Supplementary Fig. S2). ICM and TE-derived samples were concordant to each other in all instances. Moreover, euploid chromosomal complements were always confirmed in the outgrowth. Remarkably, however, for two embryos at 12 dpf, we observed no evidence of a uniform structural aberration reported in the TE biopsy. In the first instance, the blastocyst presented with a 27,Mb, 3p duplication, however a euploid profile was observed at 12 dpf (Table I, Fig. 3A). Similarly, we could not confirm a 102 Mb, 1q duplication for embryo PGT12 at 12 dpf. In this case, both the ICM and two TE-derived embryo portions all presented with euploid profiles (Table I, Fig. 3B). Finally, a third blastocyst diagnosed with a 79,Mb, 11q duplication and a 11p mosaic deletion also presented with a euploid profile at 8 dpf (Table I, Fig. 3C).

Embryos originally diagnosed as chromosomally mosaic were often viable, presenting with euploid profiles as early as 8 dpf

Interestingly, a high proportion of embryos originally diagnosed with mosaicism remained viable at 12 dpf (7 out of 12, 58%). Markedly, of these, 71% (5 out of 7) presented with normal profiles, including two embryos that were separated into ICM and TE-derived portions (Table I, Fig. 4). All 12 dpf embryo segments were euploid. Similar outcomes were observed for both numerical and structural CNVs (Table I, Fig. 4A, B, Supplementary Fig. S5). Furthermore, we could not confirm mosaicism in any 12 dpf outgrowths generated from blastocysts diagnosed with both uniform and mosaic aberrations. Here, only uniform abnormalities were detected at 12 dpf (Fig. 4C). As expected, embryos within this group showed reduced developmental potential (Fig. 2, Table I). Our analysis of a further seven blastocysts sequenced at 8 dpf revealed similar results (Table I). We observed no evidence of chromosomal heterogeneity in any of the 8 dpf embryos originally diagnosed as mosaic (Table I, Supplementary Fig. S3A,B). Most of the blastocysts investigated were low-grade mosaics, however euploid profiles were also observed when the degree of mosaicism exceeded 50% (Supplementary Fig. S3A). Interestingly, this embryo presented with two mosaic aneuploidies (Supplementary Fig. S3A).

In some instances, however, mosaicism at the blastocyst stage led to further chromosomal instability during development (Table I). Two such embryos remained viable at 12 dpf. The first presented with a mosaic trisomy 3 at the blastocyst stage, while this aberration was present in all cells at 12 dpf, in both embryonic lineages (Fig. 5A). The second blastocyst was originally diagnosed with a mosaic trisomy 4 and showed a reciprocal mosaic monosomy 4 at 12 dpf (Fig. 5B). Finally, non-viable embryos ($n = 5$) commonly presented with mosaic monosomies or deletions at the blastocyst stage (Table I, Supplementary Fig. S4). We often observed that embryos showing higher levels of mosaicism were more likely to detach during culture, although not in all cases (Supplementary Fig. S4).

PGT-A demonstrates high sensitivity, however a proportion of euploid embryos remain inadvertently diagnosed as clinically unsuitable

Based on our sequencing data, we further evaluated sensitivity and specificity in the context of PGT-A. To estimate the diagnostic accuracy of a TE biopsy in predicting the chromosomal constitution of the embryo outgrowth at 8 or 12 dpf, we used classifications such as true positive (abnormal embryo outgrowth, abnormal TE biopsy), true negative (normal embryo outgrowth, normal TE biopsy), false negative (abnormal outgrowth, normal TE biopsy) or false positive (normal embryo outgrowth, abnormal TE biopsy). Sensitivity, the probability to accurately diagnose an embryo as abnormal from a TE biopsy was 100% (19 out of 19). However, specificity, the proportion of accurately diagnosed euploid embryos classified as clinically suitable was 62% (13 out of 21), revealing a relatively high false positive rate of 38% (8 out of 21). Of these, 67% were diagnosed as chromosomally mosaic (6 out of 9). Yet, the remaining 33% (3 out of 9) presented with a uniform aberration in the TE biopsy. Overall, our findings demonstrate a

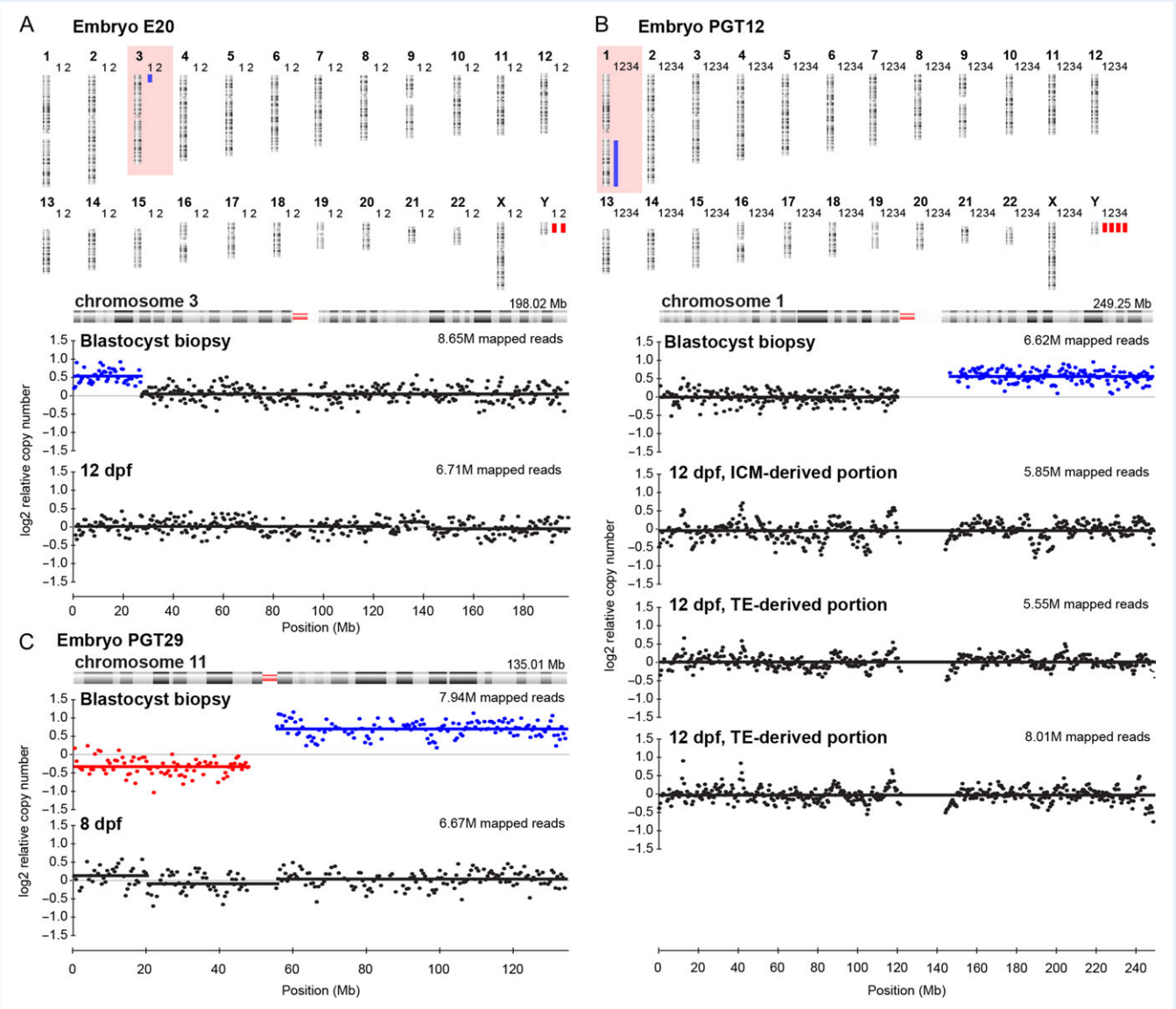

Figure 3 Uniform structural variants diagnosed at the blastocyst stage, but not confirmed 8 or 12 days post-fertilisation (dpf). Blue bars indicate duplications, red bars indicate deletions. M = million (**A**) Results for embryo E20. 1 = Blastocyst profile, 2 = 12 dpf embryo outgrowth profile. Profiles for chromosome 3 show a uniform 3p26p24.1, 27.0 Mb duplication at the blastocyst stage, while a euploid profile was observed at 12 dpf. (**B**) Results for embryo PGT12. 1 = Blastocyst profile, 2 = 12 dpf, inner cell mass (ICM)-derived embryo outgrowth portion. 3 and 4 = 12 dpf, trophectoderm (TE)-derived embryo outgrowth portions. Profiles for chromosome 1, reveal a uniform 1q21.1q44, 102.0 Mb duplication diagnosed at the blastocyst stage and euploid profiles for both ICM and TE-derived embryo portions. (**C**) Profiles for chromosome 11, embryo PGT29, reveal a 47.5Mb mosaic 11p15.5p11.2 deletion in addition to a uniform 79.0Mb, 11q11q25 duplication at the blastocyst stage, while a euploid profile was observed at 8 dpf.

diagnostic accuracy of 80% for PGT-A. Nevertheless, if structural and mosaic abnormalities are not considered, accuracy increases to 100%, with a 0% false positive and false negative rate.

Discussion

In the present study we use an extended *in vitro* embryo culture system to provide novel insights into cytogenetic (in)stability during human peri-implantation development. Good-quality blastocysts, biopsied on Day 5 or 6, were plated and cultured *in vitro* until 8 or 12 dpf. To assess the impact of chromosomal aberrations on embryogenesis, several outgrowths were selected for NGS and correlated to their original diagnosis. To our knowledge, this is the first study to assess the fate of chromosomally abnormal and mosaic human embryos cultured until 12 dpf *in vitro*, using a high-resolution sequencing approach.

Despite the high frequency of genetic instability observed in preimplantation embryos, the incidence of chromosomal aberrations becomes significantly reduced during gestation. It is thus widely recognised that most abnormalities are incompatible with live birth. During preimplantation development, both trisomies and monosomies occur

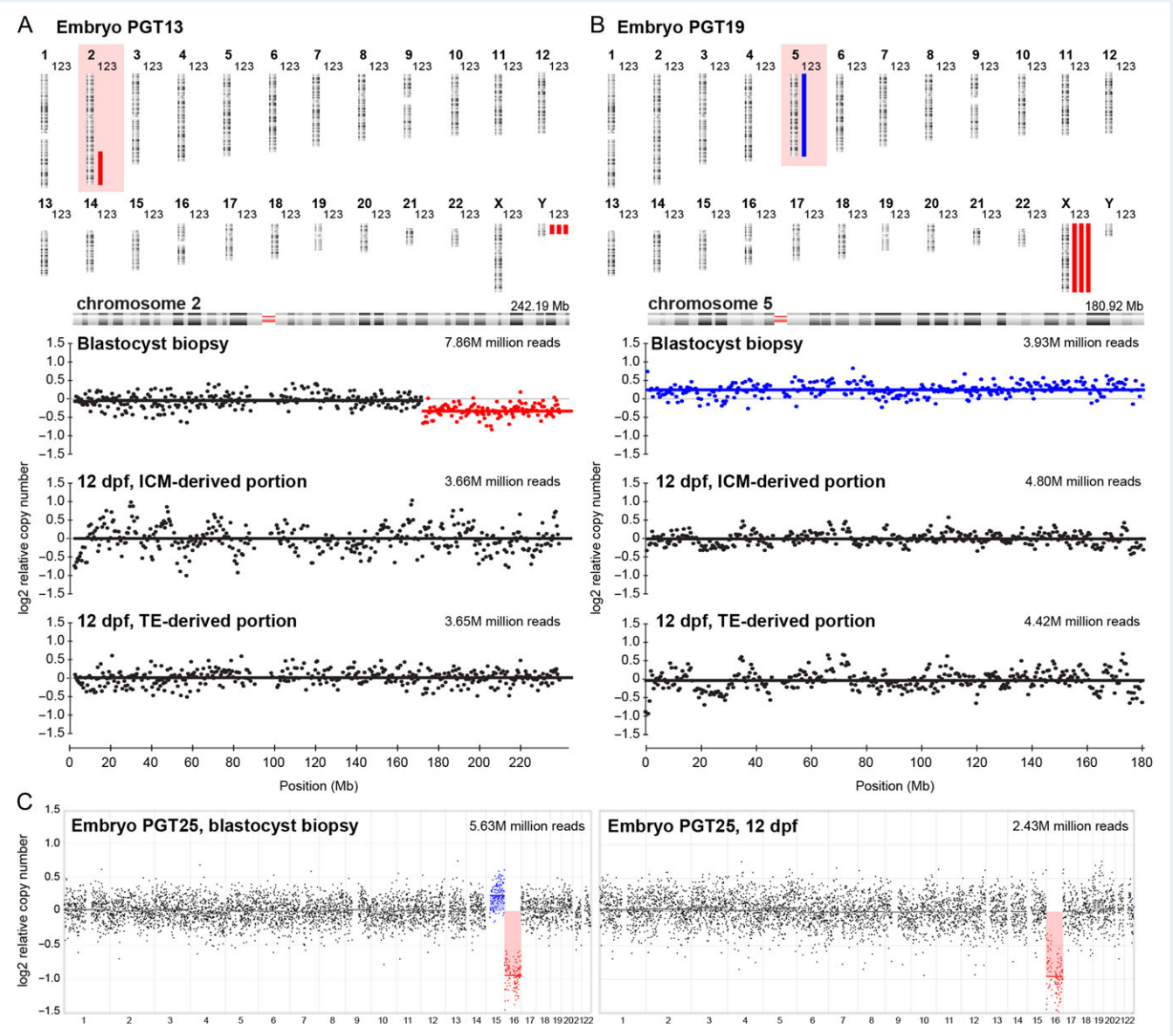

Figure 4 Mosaicism at the blastocysts stage not detected 12 days post-fertilisation (dpf). Blue bars indicate duplications, red bars indicate deletions. 1 = Blastocyst profile, 2 = 12 dpf, inner cell mass (ICM)-derived embryo outgrowth portion. 3 = 12 dpf, trophectoderm (TE)-derived embryo outgrowth portion. M = million (**A**) Results for embryo PGT13. Profiles for chromosome 2, reveal a 2q31.1q37.3, 72.5Mb mosaic deletion, while both ICM and TE-derived 12 dpf embryo portions show euploid profiles. (**B**) Results for embryo PGT19. Profiles for chromosome 5, reveal a mosaic trisomy 5, while euploid profiles were observed for both ICM and TE-derived portions of the embryo outgrowth at 12 dpf. (**C**) Line graph sequencing results for embryo PGT25. The blastocyst biopsy profile revealed a mosaic trisomy 15 in addition to a uniform monosomy 16. Only the monosomy 16 can be detected at 12 dpf.

at a relatively similar frequency, most commonly affecting chromosomes 22, 16, 21, 18 and 15 (Fragouli *et al.*, 2013). However, tissues from early miscarriages rarely show chromosomal losses, while the prevalence of trisomies remains fairly similar to that observed in preimplantation embryos (Rodriguez-Purata *et al.*, 2015). It has thus been postulated that monosomies lead to very early pregnancy loss (Goddijn and Leschot, 2000). As seen in our study, embryos with trisomies 16, 21 and 22 all remained viable at 12 dpf, while those presenting with monosomies were significantly more likely to detach after Day 8. In accordance with prenatal data, our findings suggest lethality of autosomal monosomies at the time of implantation or shortly thereafter. We reveal similar outcomes for structural aberrations, with embryos diagnosed with duplications more likely to develop to 12 dpf compared to those with deletions. Furthermore, all embryos diagnosed with multiple aberrations were non-viable at 12 dpf, attesting to the higher genetic burden of more complex chromosomal constitutions.

As with uniform abnormalities, prenatal specimens show a reduced incidence of chromosomal mosaicism (van Echten-Arends *et al.*, 2011). The higher frequency of blastocyst heterogeneity reported with the advent of NGS, has thus raised substantial controversy surrounding

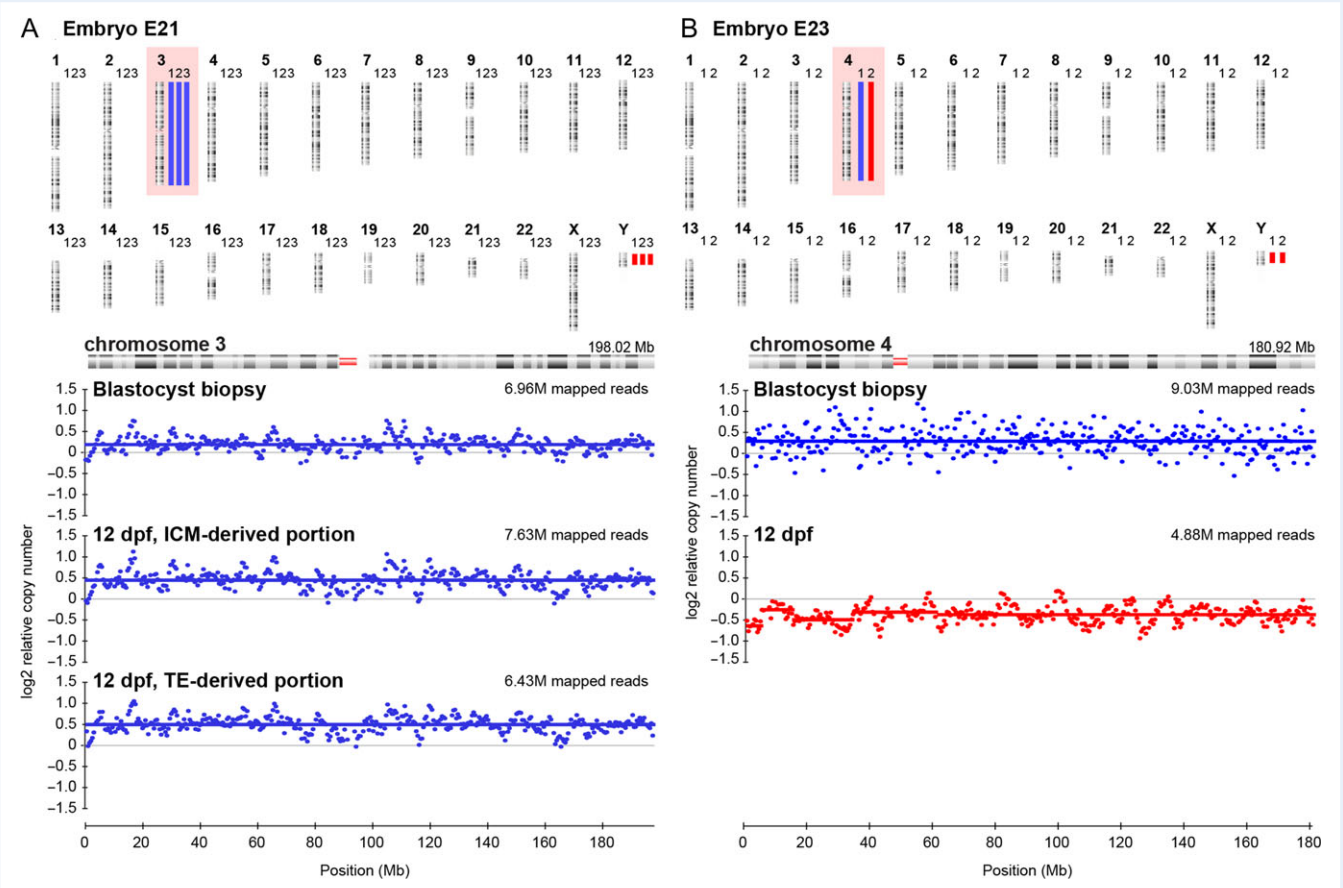

Figure 5 Mosaicism confirmed 12 days post-fertilisation (dpf). Blue bars indicate duplications, red bars indicate deletions. M = million (**A**) Results for embryo E21. 1 = Blastocyst profile, 2 = 12 dpf, inner cell mass (ICM)-derived embryo outgrowth portion. 3 = 12 dpf, trophectoderm (TE)-derived embryo outgrowth portion. Profiles for chromosome 3 reveal a mosaic trisomy 3, while both ICM and TE-derived 12 dpf embryo portions show a uniform trisomy 3. (**B**) Results for embryo E23. 1 = Blastocyst profile, 2 = 12 dpf outgrowth profile. Profiles for chromosome 4, reveal a mosaic trisomy 4, while a reciprocal mosaic monosomy 4 was observed at 12 dpf.

both the diagnosis of mosaicism, as well as the implantation potential of mosaic embryos. Goodrich *et al.*, 2017 determined variable accuracy for detecting mosaicism across several NGS analysis platforms. Our results also illustrate the technical limitations of NGS for accurately reporting mosaicism, with a misdiagnosis rate of ~18%. Distinguishing biological variability from possible technical artefacts, including amplification bias, DNA degradation and S-phase artefacts undoubtedly confounds the diagnosis of mosaicism (Capalbo *et al.*, 2017). Although NGS allows scaling, WGA remains the limiting factor in achieving higher resolution with low DNA input (Deleye *et al.*, 2015b). These aspects must be acknowledged and potentially contribute to an overestimation of chromosomal mosaicism in clinical practice. Our previous findings comparing chromosomal profiles of different portions of the blastocyst, uncovered a high sensitivity in the context of PGT-A (Popovic *et al.*, 2018). Our current data support this evaluation. All aberrations observed at 8 and 12 dpf were accurately diagnosed at the blastocyst stage, confirming the high reliability of PGT-A as a tool to select euploid embryos suitable for transfer, showing no false negative results. However, a proportion of euploid embryos remain inadvertently diagnosed as clinically unsuitable. False positive diagnoses (n = 9) were either attributed to a mosaic (6 out of 9) or structural aberration reported in the TE biopsy (3 out of 9). Although the finding of mosaicism is generally valid, overestimation will in part inevitably contribute to the reduced specificity reported. Nevertheless, attempting to accurately identify and categorise mosaic blastocysts based on a single TE biopsy also remains fundamentally unattainable due to the complex nature of chromosomal heterogeneity itself, leading to sampling bias (Popovic *et al.*, 2018).

Current data regarding clinical outcomes following the transfer of mosaic embryos remain exceptionally scarce, with just over 100 pregnancies and 50 live births reported to date (Greco *et al.*, 2015; Fragouli *et al.*, 2017; Lledó *et al.*, 2017; Spinella *et al.*, 2018). We show that some blastocysts reported as mosaic generated viable euploid outgrowths, as early as 8 dpf. Our findings correlate to clinical data, reporting comparable implantation rates for single, double and structural mosaic gains and losses (Munné *et al.*, 2017). Although, we observed, that embryos with mosaic monosomies detached more readily *in vitro*. This was the case regardless of the degree of mosaicism originally reported, possibly indicative of the added pressure of the extended *in vitro* culture system. Overall, however, mosaic blastocysts diagnosed with a higher percentage of abnormal cells were more likely to be non-viable at 12 dpf. Clinical data suggest that the load of

abnormal cells may impact the developmental fate of mosaic blastocysts (Fragouli et al., 2017; Spinella et al., 2018). Similarly, Bolton et al., 2016 reveal that mosaic embryos containing a sufficient proportion of euploid cells developed normally. Our findings may suggest the depletion of abnormal cells in the embryo outgrowths. Aneuploidy is known to decrease the rate of cell proliferation (Sheltzer and Amon, 2011). Nevertheless, the rate of mosaicism in a TE biopsy does not always reflect the rate of mosaicism for the entire blastocyst (Popovic et al., 2018). As multiple samples obtained from the same outgrowth showed concordant results in all instances, we cannot exclude the possibility that altered $\log_2$ relative copy number values may in some cases result from amplification bias, leading to over- or under-represented regions in the genome. With an aim to provide a framework for clinical care, guidelines for prioritising mosaic embryos for transfer were recently issued in two position statements (PGDIS, 2016; CoGEN, 2017). Our data uphold these guidelines, however, we reveal that thorough validation prior to diagnosing mosaicism in a clinical setting is vital.

In some instances, we observed that a mosaic diagnosis may be indicative of further genomic instability during peri-implantation. For one embryo, we observed a low-grade mosaic trisomy 3 at the blastocyst stage, while we detected this aberration in all cells, in both embryonic lineages. In this case, the possibility of misdiagnosis is relatively low. Reports of trisomy 3 are rare in blastocysts (Rodriguez-Purata et al., 2015), hence viability is likely to be compromised prior to the blastocyst stage of development, if a uniform aberration is present. Moreover, while WGA can introduce a representation bias for smaller genomic segments, under-representation of an entire chromosome is very unlikely (Deleye et al., 2015a). For a further embryo, we observed reciprocal mosaic abnormalities at the blastocyst stage and 12 dpf. Reciprocal chromosomal errors reveal strong evidence of a mitotic non-disjunction event, a striking example of embryo mosaicism. Here, we reveal that the reciprocal aberration associated with a higher level of risk may persist within the embryo, ultimately leading to negative clinical outcomes. Nonetheless, studying human peri-implantation events remains exceptionally challenging. Established models omit the requirement of endometrial tissues and hence do not account for trophoblast-endometrial interactions. Additionally, estimating mosaicism will inevitably be influenced by the number of cells analysed. Our embryo outgrowths contain numerous cells, therefore detecting low levels of mosaicism, when a significantly higher number of euploid cells are present, will not be possible.

Overall, our findings demonstrate that distinguishing technical bias from biological variability in a TE biopsy will remain a challenge with current WGA protocols. This will inherently limit the accuracy of diagnosing mosaicism in clinical practice. As such, a certain proportion of euploid embryos will inevitably be reported as clinically unsuitable, while a portion of mosaic blastocysts will lead to negative clinical outcomes following transfer. Our findings stress that comprehensive validation of NGS platforms, as well as rigorous data interpretation is imperative when reporting chromosomal mosaicism. In addition, modelling genetic instability *in vitro* may deliver a more fundamental approach for evaluating the clinical implications of chromosomal mosaicism, serving as a prelude to future follow-up studies of clinical outcomes. Above all, the biological and methodological drawbacks of diagnosing mosaicism must be recognised and carefully communicated to all patients undergoing PGT-A.

Supplementary data

Supplementary data are available at *Human Reproduction* online.

Acknowledgements

We thank all patients of the Department for Reproductive Medicine, Ghent University Hospital, for donating their cryopreserved embryos for this study. We further wish to thank Machteld Baetens, Tine De Pretre and Melek Yörük for their assistance in the sequencing experiments. This research has been conducted through a collaboration with the Bimetra biobank, a high-quality bio-repository for the Ghent University Hospital and Ghent University.

Authors' roles

M.P. contributed to the conception and design of the study, performed experiments, acquired and analysed data and wrote the article. L.D., J. T., A.D. and B.M. analysed data. M.B. and S.M.C.d.S.L. assisted in the establishment and validation of the extended *in vitro* embryo culture system. Critical revisions were given by P.D.S., S.M.C.d.S.L, B.M. and B.H. All authors contributed to the interpretation of the results and reviewed the article.

Funding

This research is funded by the Ghent University Special Research Fund, Bijzonder Onderzoeksfonds (BOF01D08114) awarded to M.P., the Research Foundation—Flanders (FWO.KAN.0005.01) research grant awarded to B.H. and De Snoo-van 't Hoogerhuijs Stichting awarded to S.M.C.d.S.L. We would like to thank Ferring Pharmaceuticals (Aalst, Belgium) for an unrestricted educational grant. The authors declare no competing interests.

Conflict of interest

None declared.

References

van den Berg MMJ, van Maarle MC, van Wely M, Goddijn M. Genetics of early miscarriage. *Biochim Biophys Acta* 2012;**1822**:1951–1959.

Bolton H, Graham SJL, Aa N, Van der, Kumar P, Theunis K, Fernandez Gallardo E, Voet T, Zernicka-Goetz M, Gallardo EF, Voet T *et al*. Mouse model of chromosome mosaicism reveals lineage-specific depletion of aneuploid cells and normal developmental potential. *Nat Commun* 2016; **7**:11165.

Bontekoe S, Mantikou E, van Wely M, Seshadri S, Repping S, Mastenbroek S. Low oxygen concentrations for embryo culture in assisted reproductive technologies. *Cochrane Database Syst Rev.* 2012;**7**:CD008950

Capalbo A, Ubaldi FM, Rienzi L, Scott R, Treff N. Detecting mosaicism in trophectoderm biopsies: current challenges and future possibilities. *Hum Reprod* 2017;**32**:492–498.

CoGEN. Controversies in Preconception, Preimplantation and Prenatal Genetic Diagnosis (CoGEN) Statement - IVF-Worldwide. 2017; https://ivf-worldwide.com/cogen/general/cogen-statement.html.

Deglincerti A, Croft GF, Pietila LN, Zernicka-Goetz M, Siggia ED, Brivanlou AH. Self-organization of the *in vitro* attached human embryo. *Nature* 2016;**533**:1–13.

Deleye L, De Coninck D, Christodoulou C, Sante T, Dheedene A, Heindryckx B, Van Den Abbeel E, De Sutter P, Menten B, Deforce D *et al*. Whole genome amplification with SurePlex results in better copy number alteration detection using sequencing data compared to the MALBAC method. *Sci Rep* 2015a;**5**:11711.

Deleye L, Dheedene A, De Coninck D, Sante T, Christodoulou C, Heindryckx B, Van Den Abbeel E, De Sutter P, Deforce D, Menten B *et al*. Shallow whole genome sequencing is well suited for the detection of chromosomal aberrations in human blastocysts. *Fertil Steril* 2015b; **104**:1276–1285.

Fragouli E, Alfarawati S, Spath K, Babariya D, Tarozzi N, Borini A, Wells D. Analysis of implantation and ongoing pregnancy rates following the transfer of mosaic diploid–aneuploid blastocysts. *Hum Genet* 2017;**136**:805–819.

Fragouli E, Alfarawati S, Spath K, Jaroudi S, Sarasa J, Enciso M, Wells D. The origin and impact of embryonic aneuploidy. *Hum Genet* 2013;**132**: 1001–1013.

Gardner, DK and Schoolcraft, WB. (1999) In Vitro Culture of Human Blastocyst. In: Jansen, R and Mortimer, D., Eds., *Towards Reproductive Certainty: Infertility and Genetics Beyond*, Parthenon Press, Carnforth, 377–388.

Goddijn M, Leschot NJ. Genetic aspects of miscarriage. *Best Pract Res Clin Obstet Gynaecol* 2000;**14**:855–865.

Goodrich D, Xing T, Tao X, Lonczak A, Zhan Y, Landis J, Zimmerman R, Scott RT, Treff NR, Treff NR. Evaluation of comprehensive chromosome screening platforms for the detection of mosaic segmental aneuploidy. *J Assist Reprod Genet* 2017;**34**:975–981.

Greco E, Minasi MG, Fiorentino F. Healthy babies after intrauterine transfer of mosaic aneuploid blastocysts. *N Engl J Med* 2015;**373**:2089–2090.

Harper JC, Wilton L, Traeger-Synodinos J, Goossens V, Moutou C, SenGupta SB, Pehlivan Budak T, Renwick P, De Rycke M, Geraedts JPM *et al*. The ESHRE PGD consortium: 10 years of data collection. *Hum Reprod Update* 2012;**18**:234–247.

Lledó B, Morales R, Ortiz JA, Blanca H, Ten J, Llácer J, Bernabeu R. Implantation potential of mosaic embryos. *Syst Biol Reprod Med* 2017; **63**:206–208.

Maxwell SM, Colls P, Hodes-Wertz B, McCulloh DH, McCaffrey C, Wells D, Munné S, Grifo JA. Why do euploid embryos miscarry? A case-control study comparing the rate of aneuploidy within presumed euploid embryos that resulted in miscarriage or live birth using next-generation sequencing. *Fertil Steril* 2016;**106**:1414–1419.

Mertzanidou A, Wilton L, Cheng J, Spits C, Vanneste E, Moreau Y, Vermeesch JR, Sermon K. Microarray analysis reveals abnormal chromosomal complements in over 70% of 14 normally developing human embryos. *Hum Reprod* 2013;**28**:256–264.

Munné S, Blazek J, Large M, Martinez-Ortiz PA, Nisson H, Liu E, Tarozzi N, Borini A, Becker A, Zhang J *et al*. Detailed investigation into the cytogenetic constitution and pregnancy outcome of replacing mosaic blastocysts detected with the use of high-resolution next-generation sequencing. *Fertil Steril* 2017;**108**:62–71.e8.

Munné S, Wells D. Detection of mosaicism at blastocyst stage with the use of high-resolution next-generation sequencing. *Fertil Steril* 2017;**107**: 1085–1091.

PGDIS. PGDIS position statement on chromosome mosaicism and preimplantation aneuploidy testing at the blastocyst stage. 2016; http://www.pgdis.org/docs/newsletter_071816.html.

Popovic M, Dheedene A, Christodoulou C, Taelman J, Dhaenens L, Van Nieuwerburgh F, Deforce D, Van den Abbeel E, De Sutter P, Menten B *et al*. Chromosomal mosaicism in human blastocysts: the ultimate challenge of preimplantation genetic testing? *Hum Reprod* 2018;**33**:1342–1354.

Refaat B, Ledger W. The expression of activins, their type II receptors and follistatin in human Fallopian tube during the menstrual cycle and in pseudo-pregnancy. *Hum Reprod* 2011;**26**:3346–3354.

Rodriguez-Purata J, Lee J, Whitehouse M, Moschini RM, Knopman J, Duke M, Sandler B, Copperman A. Embryo selection versus natural selection: how do outcomes of comprehensive chromosome screening of blastocysts compare with the analysis of products of conception from early pregnancy loss (dilation and curettage) among an assisted reproductive technology population? *Fertil Steril* 2015;**104**:1460–1466.e12.

Rossant J, Tam PPLL. New insights into early human development: lessons for stem cell derivation and differentiation. *Cell Stem Cell* 2017;**20**:18–28.

Sachdev NM, Maxwell SM, Ribustello L, Liu E, McCulloh DH, Munne S, Grifo J. The high rate of abnormal embryos in donor cycles is reflected in donor oocyte pregnancy outcomes. *Fertil Steril* 2016;**106**:e150–e151.

Sante T, Vergult S, Volders P-J, Kloosterman WP, Trooskens G, De Preter K, Dheedene A, Speleman F, De Meyer T, Menten B. ViVar: a comprehensive platform for the analysis and visualization of structural genomic variation. *PLoS One* 2014;**9**:e113800.

Scheinin I, Sie D, Bengtsson H, Wiel MA, van de, Olshen AB, Thuijl HF, van, Essen HF, van, Eijk PP, Rustenburg F, Meijer GA *et al*. DNA copy number analysis of fresh and formalin-fixed specimens by shallow whole-genome sequencing with identification and exclusion of problematic regions in the genome assembly. *Genome Res* 2014;**24**:2022–2032.

Schindelin J, Arganda-Carreras I, Frise E, Kaynig V, Longair M, Pietzsch T, Preibisch S, Rueden C, Saalfeld S, Schmid B *et al*. Fiji: an open-source platform for biological-image analysis. *Nat Methods* 2012;**9**:676–682.

Shahbazi MN, Jedrusik A, Vuoristo S, Recher G, Hupalowska A, Bolton V, Fogarty NME, Campbell A, Devito LG, Ilic D *et al*. Self-organization of the human embryo in the absence of maternal tissues. *Nat Cell Biol* 2016;**18**:700–708.

Sheltzer JM, Amon A. The aneuploidy paradox: costs and benefits of an incorrect karyotype. *Trends Genet* 2011;**27**:446–453.

Spinella F, Fiorentino F, Biricik A, Bono S, Ruberti A, Cotroneo E, Baldi M, Cursio E, Minasi MG, Greco E. Extent of chromosomal mosaicism influences the clinical outcome of *in vitro* fertilization treatments. *Fertil Steril* 2018;**109**:77–83.

van Echten-Arends J, Mastenbroek S, Sikkema-Raddatz B, Korevaar JC, Heineman MJ, van der Veen F, Repping S. Chromosomal mosaicism in human preimplantation embryos: a systematic review. *Hum Reprod Update* 2011;**17**:620–627.

Van Landuyt L, Verpoest W, Verheyen G, De Vos A, Van De Velde H, Liebaers I, Devroey P, Van Den Abbeel E. Closed blastocyst vitrification of biopsied embryos: evaluation of 100 consecutive warming cycles. *Hum Reprod* 2011;**26**:316–322.

Vera-Rodriguez M, Rubio C. Assessing the true incidence of mosaicism in preimplantation embryos. *Fertil Steril* 2017;**107**:1107–1112.